Twisted Bessel Beams via Bull-Eye Antennas Excited by a Single Uniform Circular Array

Davide Comite, *Senior Member, IEEE,* Walter Fuscaldo, *Member, IEEE,* Giancarlo Merola, Paolo Burghignoli, *Senior Member, IEEE,* Paolo Baccarelli, *Member, IEEE,* and Alessandro Galli, *Member, IEEE*

***Abstract*—The design of a microstrip bull-eye antenna operating at microwave frequencies and excited by a single uniform circular array of vertical coaxial probes is presented. The array feeder excites higher order cylindrical leaky waves with a fast, backward, radially propagating space harmonic capable of generating twisted Bessel beams in the near-field region. By varying the phasing of the sources, beams with consistent axicon angles and different azimuthal orders can be synthesized, corresponding to different orbital-angular-momentum (OAM) states. A careful design of the feeder allows for obtaining Bessel-like field distributions in the radiative near field and stable far-field patterns as a function of the azimuth angle, as well as satisfactory matching at the input ports, both in terms of passive scattering coefficients and of active reflection coefficients, for five different OAM states. Numerical full-wave results are reported to validate the proposed design for microwave applications.**

***Index Terms*—Bessel beams, twisted beams, orbital angular momentum, leaky waves, planar antennas, array feeders.**

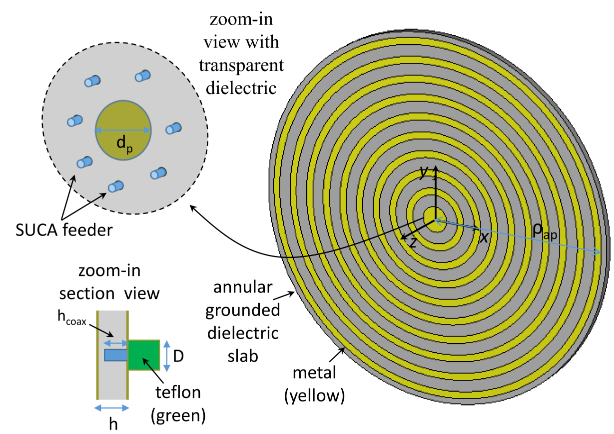

Fig. 1. Bull-Eye antenna (BE) fed by a single uniform circular array (SUCA) of vertical coaxial probes.

I. Introduction and Background

TWISTED beams, i.e., electromagnetic waves carrying orbital angular momentum (OAM), are currently under intense investigation as a means of providing improved performance in near-field communication and remote sensing systems (see, e.g., [1]–[5], and references therein). Of particular interest, in this context, are nondiffracting beams, such as Bessel beams (BBs), which exhibit limited-diffraction spreading within a finite distance from the radiating aperture (the *nondiffracting range*) [6].

Twisted BBs have an azimuthal dependence $\exp(j\ell\phi)$, where ϕ is the angular coordinate in a (ρ, ϕ, z) cylindrical reference frame whose z-axis is the propagation axis of the beam and ℓ is the azimuthal (or OAM) order of the beam. They have been synthesized so far by using metasurfaces [7]–[10], arrays [11], lenses [12], and radial-line slot arrays (RLSAs) [13]–[15]; the latter have also been considered for producing twisted X-waves as polychromatic superposition of twisted BBs [16]. On the other hand, several structures have also been proposed to generate OAM beams in the far field, such as, e.g., resonant helical antennas [17], arrays [18], and metasurfaces [19], [20]. Multimode and multifed patch antennas have also been proposed [21], [22], whereas in [23] the topological properties of vortex fields generated by higher order modes supported by circular patch antennas are investigated.

Backward cylindrical leaky waves (CLWs) supported by radially periodic planar structures provide an alternative and versatile route for the generation of shaped near-field distributions and focused beams [24]–[26]. In this framework, we present the design of a bull-eye (BE) radially periodic microstrip antenna excited by a single uniform circular array (SUCA), as shown in Fig. 1. SUCAs have recently been proposed in [27] as feeders for Fabry–Perot cavity antennas operating on higher order CLWs (HOCLWs) of the *forward* type [28], which produce twisted conical far-field patterns but rapidly diverging near-field distributions. Here we exploit the radial periodicity of the BE to excite *backward* HOCLWs capable of producing twisted BBs with variable OAM order both in the near and far field. Preliminary results based on ideal dipole sources have been presented in [29]. In this Letter, we provide a complete and detailed description of the near field supported by the antenna, employ realistic vertical coaxial probes, and address the nontrivial problem of the array matching at the input ports. By suitably optimizing the array parameters, the efficient excitation of BBs with five different OAM orders ($\ell = 0, \pm1, \pm2$) is achieved with very good passive parameters and input reflection coefficients as well as stable conical radiation in the far field.

D. Comite, G. Merola, P. Burghignoli, and A. Galli are with the Department of Information Engineering, Electronics and Telecommunications, Sapienza University of Rome, Via Eudossiana 18, 00184 Rome, Italy. *Corresponding author: Davide Comite*. (email: davide.comite@uniroma1.it)

W. Fuscaldo is with Istituto per la Microelettronica e Microsistemi (CNR-IMM), Via del fosso cavaliere 100, 00133 Rome, Italy.

P. Baccarelli is with the Department of Engineering, Roma Tre University, via Vito Volterra 62, 00146 Rome, Italy.

II. Structure Description

The initial configuration of the proposed BE antenna, shown in Fig. 1, is constituted by a central circular patch of diameter

$d_\mathrm{p} = 5$ mm surrounded by $N_\mathrm{ring} = 13$ concentric microstrip rings of width $w = 4$ mm and spacing $s = 6$ mm, printed on a grounded dielectric slab having thickness $h = 3.14$ mm and relative permittivity $\varepsilon_\mathrm{r} = 2.2$.

The numerical values of the antenna parameters are chosen as in [30], [31], so that the linearized structure supports a fundamental leaky TM Bloch mode whose $n = -1$ space harmonic is in a backward radiative regime between 13.5 and about 23 GHz. The relevant dispersion curve, obtained with an in-house method-of-moments code is not reported here for space limitation, but can be found in [30], [31]. With this choice of parameters, by operating at $f = 18$ GHz, the value of the normalized phase constant for the radiative space harmonic is $\beta/k_0 \simeq -0.4$, corresponding to a leaky-wave emission angle $\theta_\mathrm{LW} \simeq 23.6°$, whereas the normalized attenuation constant is $\alpha/k_0 \simeq 0.03$. Since the radius of the antenna aperture is $\rho_\mathrm{ap} = 140$ mm, by taking into account the exponential decay factor $\exp(-\alpha\rho)$ as well as the cylindrical-wave algebraic spreading factor $\rho^{-1/2}$, the amplitude decay from the edge of the central disk $d_\mathrm{p}/2$ to the edge of the aperture $\rho = \rho_\mathrm{ap}$ is about 96%. As shown in [25], [30], the excitation of a cylindrical leaky wave with a backward radiative space harmonic, excited by a single coaxial cable placed in the geometric center of the structure, gives rise to a BB with axicon angle θ_LW within a diamond-shaped region with apexes on the z-axis at $z = 0$ and at $z = z_\mathrm{NDR}$, where $z_\mathrm{NDR} = \rho_\mathrm{ap} \cot\theta_\mathrm{LW} \simeq 320.8$ mm is the nondiffracting range.

Here the BE antenna is excited by a SUCA with radius a of N coaxial probes having length h_coax. (This will be reported later on as it will be finely tuned to optimize the impedance matching). The coaxial ports have outer diameter $D = 0.9906$ mm, inner diameter $d = 0.3048$ mm, and inner dielectric with relative permittivity 2.1 (Teflon), all values that are commercially available (the part number can be found in [30]). Practical realizations of the coaxial feeder are reported in [18], [30], [32], whereas an array has been manufactured in [33]. By letting the complex excitation coefficients of the array elements be $I_i = I_0 \exp(-j(i-1)\ell 2\pi/N)$ $(i = 1, \ldots, N)$, a higher order BB can be excited with OAM order equal to ℓ and a common axicon angle independent of ℓ. This is a remarkable feature: in free space a SUCA would produce patterns of the kind $J_\ell(k_0 a \sin\theta)$, whose beam angle is determined by the first maximum of the Bessel function $J_\ell(\cdot)$, which increases with ℓ; here the aperture field is established by a leaky wave, hence the beam angle depends on the phase constant of such a wave and is almost independent of ℓ, at least for small ℓ (more details can be found in [27]).

III. Antenna Design and Validations

A. Antenna Design

The SUCA feeder parameters, i.e., the number of coaxial probes N, the radius of the array a, and the length of the coaxial probes h_coax, have been determined considering two design goals: *i*) the *purity* of excitation of the desired OAM orders, in this case $|\ell| \leq \ell_\mathrm{max} = 3$, in terms of both amplitude and phase; *ii*) the matching performance at the input ports.

As concerns the OAM purity, i.e., the relative level of excitation of the desired azimuthal order ℓ and of the undesired higher order harmonics $\ell + nN$ $(n = \pm 1, \pm 2, \ldots)$, this is directly affected by the values of N and a. Guidelines for dimensioning these parameters were presented in [28]; these, however, apply to SUCAs placed inside Fabry–Perot cavity antennas, which are uniform structures in the plane transverse to z, and thus cannot be applied directly to the BE, which is not translationally invariant in the same plane. In other words, changing the radius of the SUCA the radiation performance of the array will be affected, due to the different interaction between the sources and the metallic strips. Therefore, a numerical study of the field excited by SUCAs with different values of N and a has been carried out using CST Microwave Studio, aimed at letting the amplitude oscillations of the far field along the cone of maximum radiation $\theta = \theta_\mathrm{LW}$ be limited within 3 dB and the phase of the field be reasonably linear as a function of the azimuthal angle ϕ. In fact, both the stability of the amplitude and the linearity of the phase provide an indirect evidence of the OAM purity of the beam. Since the characteristics of the radiated fields do not depend on the detailed constitution of the array elements, these can be replaced with ideal vertical electric dipoles, to speed up the computations. We have verified that no significant differences are observed in the far-field patterns by using realistic coaxial probes. We just note that extensive experimental validations for this feeding mechanism, working both in the far and near field, have been provided in [30], [31].

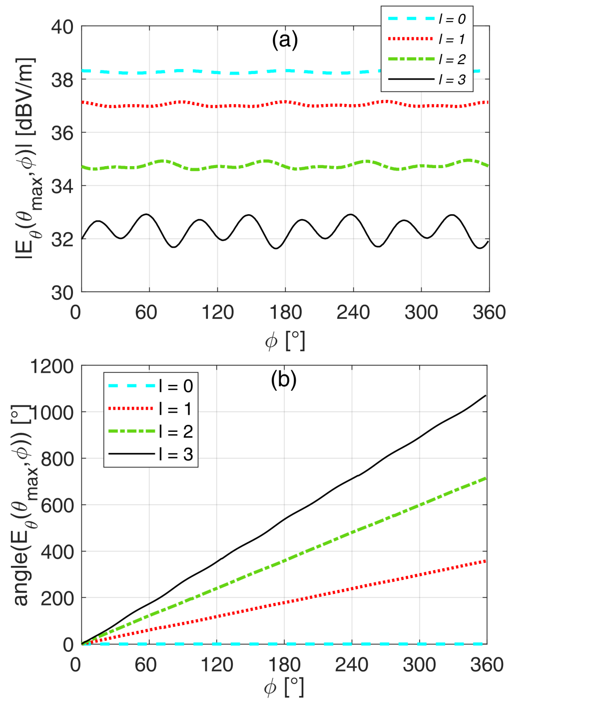

Fig. 2. Electric far field E_θ along the cone of maximum radiation $\theta = \theta_\mathrm{LW}$ as a function of the azimuthal angle ϕ, for different azimuthal orders $|\ell| \leq \ell_\mathrm{max} = 3$. (a) magnitude; (b) phase.

As a result of this study, the values $N = 8$ and $a = 6$ mm have been selected; as shown in Fig. 2, the expected performance is achieved both in terms of amplitude omni-directionality and phase linearity for all the desired azimuthal orders. The reported values refer to the co-polar, vertically

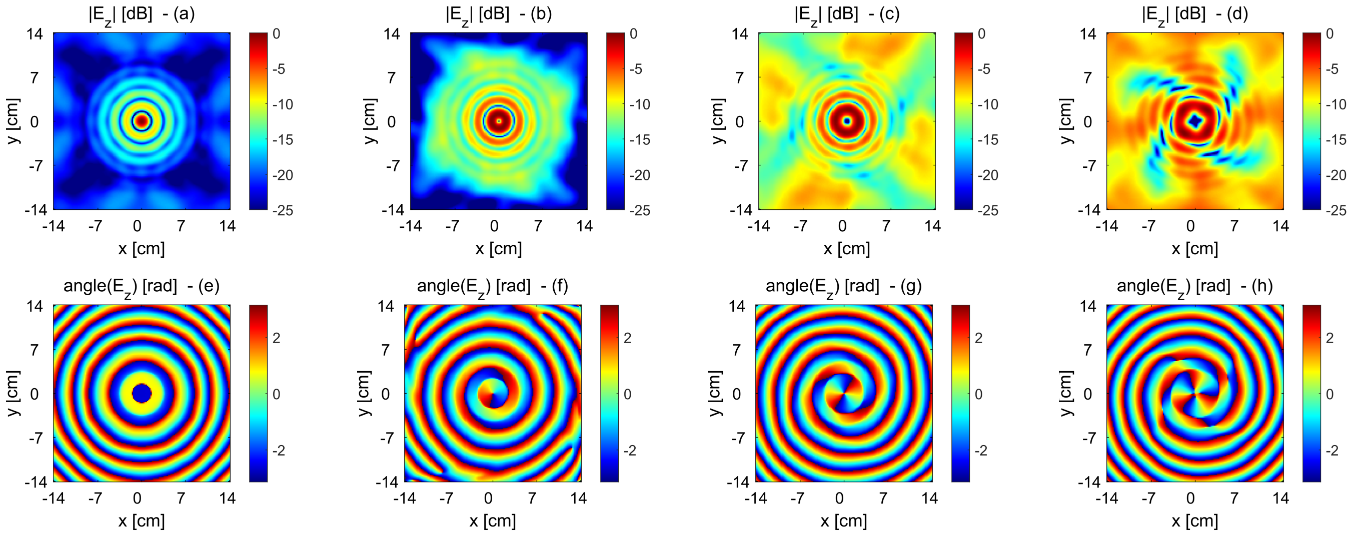

Fig. 3. Colormaps of the near field E_z (normalized, in dB) on the transverse plane $z = z_{\mathrm{NDR}}/2 \simeq 160.4$ mm for the azimuthal orders $\ell = 0, 1, 2, 3$. (a)−(d) Magnitude; (e)−(h) phase.

polarized component E_θ of the electric field only, since the cross-polar component E_ϕ, mainly generated by diffraction at the truncation, is ≥ 10 dB lower and hence can be neglected.

The input matching of the array has been studied considering both the passive scattering parameters S_{ij} and the active reflection coefficients F_i $(i, j = 1, \ldots, N)$. The azimuthal symmetry of the configuration is such that the scattering matrix is circulant, hence a single row (e.g., $S_{1j}, j = 1, \ldots, N$) needs to be studied, and the active reflection coefficients are equal for all the ports: $F_i = F_1$, $(i = 2, \ldots, N)$.

We optimized the structure design to achieve passive reflection coefficients lower than -15 dB and active reflection coefficients lower than -10 dB in magnitude. To this aim, an extensive parametric full-wave analysis of the actual probe-fed BE has been carried out in CST Microwave Studio, by varying the two design parameters d_{p} and h_{coax}. The desired performance has been achieved with $d_{\mathrm{p}} = 10$ mm and $h_{\mathrm{coax}} = 3.1$ mm for the OAM orders $|\ell| \leq 2$. In the next subsection, numerical results will be presented for the resulting BE antenna, in order to illustrate the quality of the radiated BB and the level of input matching.

B. Full-Wave Results

In Fig. 3 colormaps of the near-field distributions in the transverse plane $z = z_{\mathrm{NDR}}/2 \simeq 160.4$ mm are reported in magnitude and phase for the vertical component of the electric field (i.e., E_z), produced by the proposed BE antenna excited on the OAM orders $\ell = 0, 1, 2, 3$. The amplitude maps confirm the omnidirectionality of the radiated beams within their central core region, whereas the phase maps the twisted nature of the beams. The near field appears slightly less focused for $l = 3$ due to the finite number of sources, also confirmed by the minor oscillation visible in Fig. 2.

In Fig. 4 the amplitude profiles of E_z on the same transverse plane are reported as a function of the radial distance ρ for $\phi = 0°$ and $\phi = 90°$, along with the profile of an ideal BB having axicon angle $\theta = \theta_{\mathrm{LW}}$. It can be seen that the ideal profile is perfectly reproduced in the central part of the beam,

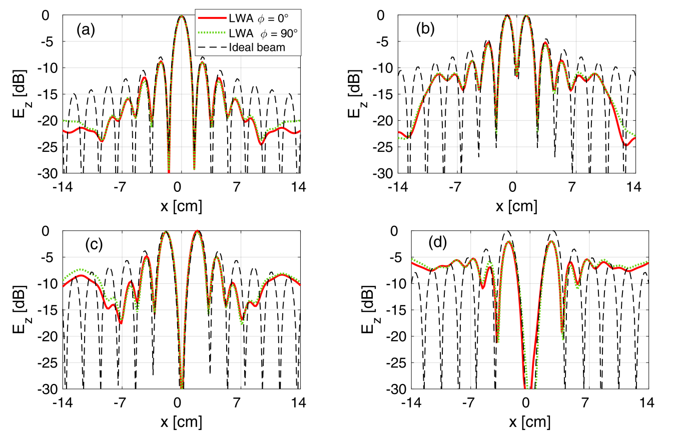

Fig. 4. Radial profiles of E_z (in magnitude) on the transverse plane $z = z_{\mathrm{NDR}}/2 \simeq 160.4$ mm along the directions $\phi = 0, 90°$, compared with the ideal BB profiles, for the different azimuthal orders: (a) $\ell = 0$, (b) $\ell = 1$, (c) $\ell = 2$, (d) $\ell = 3$.

i.e., for $\rho \leq 30$ mm, for the OAM orders $\ell = 0, 1, 2$, whereas, again, the agreement is slightly worse for $\ell = 3$. We also note that ray-optics predicts that at $z = z_{\mathrm{NDR}}$ a Bessel-like radial profile is expected to be recovered for $\rho < \rho_{\mathrm{ap}}/2 = 7$ mm [30]. For all orders, outside this central region the observed profile progressively departs from the ideal one, due to unavoidable diffraction effects of the finite lateral size of the antenna.

Figures 5(a)−(d) report the near-field distributions of the magnitude of E_z over the xz plane, again for the OAM orders $\ell = 0, 1, 2, 3$. As is manifest, the field does not undergo diffractive spreading up to the NDR of the structure. Also, for $\ell \neq 0$ a null is well defined along the z axis, which broadens for increasing ℓ. This feature is also visible in far field and it is a recognized issue for some applications [34]. Figures 5(e)-(h) present the corresponding phase distributions, where the phase progression along the z direction and the expected discontinuity of 180° at the field nulls are seen.

Figures 6(a)−(h) report the near-field distributions of the magnitude of H_z over the xz plane for three different orders

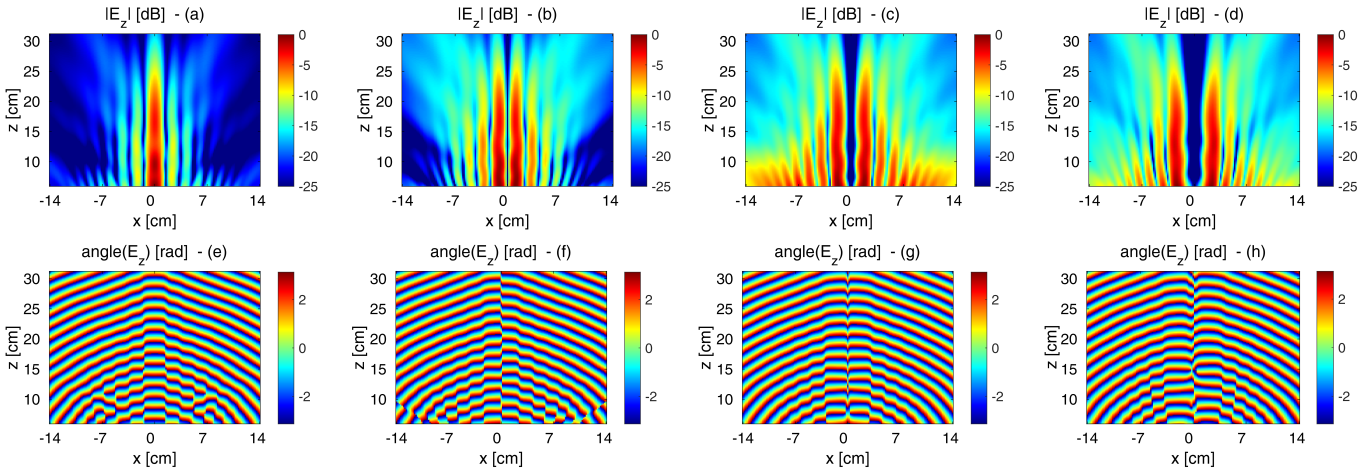

Fig. 5. Different azimuthal orders $|\ell| \leq \ell_{\max} = 3$ as in Fig. 3 but over a longitudinal plane: (a) magnitude $\ell = 0$, (b) magnitude $\ell = 1$, (c) magnitude $\ell = 2$, (d) magnitude $\ell = 3$; (e) phase $\ell = 0$, (f) phase $\ell = 1$, (g) phase $\ell = 2$, (h) phase $\ell = 3$.

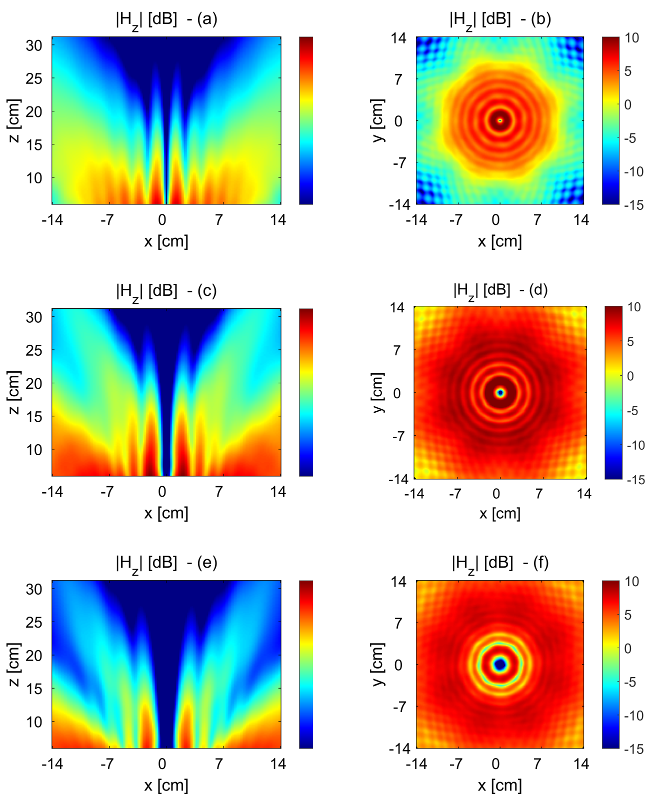

Fig. 6. Colormaps of the near field H_z (amplitude, in dB) on the longitudinal plane $z = z_{\mathrm{NDR}}/8$ (sub-figures a, c, e) and transverse plane (sub-figures b, d, f) for the azimuthal orders $\ell = 1, 2, 3$ (panels from top to bottom).

(i.e., $\ell = 1, 2, 3$). $\ell = 0$ is not reported as the field is purely TM and H_z is null. Conversely, the phasing of more sources introduces a cross-polar (TE) component, hence H_z is excited, whose intensity depends on the order ℓ (stronger for higher ℓ). As seen in Fig. 6, the magnetic field is still focused in the near field, but vanishes before reaching the NDR. This is not true for H_ϕ (not shown here for space limitations), which instead follows the same near-field patterns of the electric field.

As concerns the input matching at the array ports, in Table I the passive scattering parameters S_{1j} $(j = 1, \ldots, 8)$ are reported in magnitude: the input reflection coefficient S_{11} is below -10 dB, as are the mutual coupling coefficients S_{1j} $(j = 2, \ldots, 8)$. The resulting active reflection coefficients for the considered OAM orders are reported in Table II. It can be seen that for the five OAM orders $\ell = 0, \pm1, \pm2$ excellent values below the -10 dB threshold have been obtained, whereas the order $\ell = \pm3$ are highly mismatched.

TABLE I
SCATTERING PARAMETERS AT THE SUCA PORTS (MAGNITUDE, DB).

S_{11}	S_{12}	S_{13}	S_{14}	S_{15}	S_{16}	S_{17}	S_{18}
-12.9	-12.1	-14.6	-21.2	-19.4	-21.2	-14.6	-12.1

TABLE II
MAGNITUDE OF THE ACTIVE REFLECTION COEFFICIENTS AT THE SUCA PORTS (IN DB), FOR THE OAM ORDERS $\ell = 0, \pm1, \pm2, \pm3$.

	$\ell = 0$	$\ell = 1$	$\ell = 2$	$\ell = 3$
F	-11.5	-11.1	-15.2	-2.9

This aspect does not fully compromise the radiating performance, as the near-field distribution still matches the expected ideal magnitude and phase of the $\ell = 3$ OAM beam (see Fig. 5(d) and (h), and Fig. 6(e) and (f)). Finally it is worth noting that the active reflection coefficients for the $\ell = 0, \pm1, \pm2$ orders are maintained below -10 dB over more than 600-MHz bandwidth centered around 18 GHz: a noteworthy result in the context of simultaneous excitation of OAM beams [15].

IV. CONCLUSION

We have proposed the design of a radially periodic printed leaky-wave antenna fed by an array of sources, capable of simultaneously exciting higher order Bessel beams, therefore carrying orbital angular momentum through a nondiffracting wave. A design method is described that cannot leverage on translational invariance, as the top annular metal strip grating cannot be homogenized, but that is compact, simple to manufacture, and low cost. In principle, following the proposed approach, further optimization to support more angular momentum orders, both at microwaves and millimeter waves, can be reached. The antenna can generate vortex waves both in the far and near field, representing an attractive solution for radar imaging and next-generation communication protocols.

References

[1] M. Veysi, C. Guclu, F. Capolino, and Y. Rahmat-Samii, "Revisiting orbital angular momentum beams: Fundamentals, reflectarray generation, and novel antenna applications," *IEEE Antennas Propag. Mag.*, vol. 60, no. 2, pp. 68–81, Feb. 2018.

[2] R. Gaffoglio, A. Cagliero, G. Vecchi, and F. P. Andriulli, "Vortex waves and channel capacity: Hopes and reality," *IEEE Access*, vol. 6, pp. 19 814–19 822, 2017.

[3] Y. Chen, S. Zheng, X. Jin, H. Chi, and X. Zhang, "Single-frequency computational imaging using OAM-carrying electromagnetic wave," *J. App. Phys.*, vol. 121, no. 18, p. 184506, 2017.

[4] Y. Lei, Y. Yang, Y. Wang, K. Guo, Y. Gong, and Z. Guo, "Throughput performance of wireless multiple-input multiple-output systems using OAM antennas," *IEEE Wireless Communications Lett.*, 2020.

[5] A. Trichili, K.-H. Park, M. Zghal, B. S. Ooi, and M.-S. Alouini, "Communicating using spatial mode multiplexing: Potentials, challenges, and perspectives," *IEEE Comm. Surveys & Tutorials*, vol. 21, no. 4, pp. 3175–3203, 2019.

[6] M. Ettorre, S. C. Pavone, M. Casaletti, M. Albani, A. Mazzinghi, and A. Freni, "Near-field focusing by non-diffracting Bessel beams," in *Aperture Antennas for Millimeter and Sub-Millimeter Wave Applications*. Cham, Switzerland. Springer, 2018, pp. 243–288.

[7] M. L. Chen, L. J. Jiang, and E. Wei, "Quasi-continuous metasurfaces for orbital angular momentum generation," *IEEE Antennas Wireless Propag. Lett.*, vol. 18, no. 3, pp. 477–481, 2019.

[8] H. Shi, L. Wang, G. Peng, X. Chen, J. Li, S. Zhu, A. Zhang, and Z. Xu, "Generation of multiple modes microwave vortex beams using active metasurface," *IEEE Antennas Wireless Propag. Lett.*, vol. 18, no. 1, pp. 59–63, 2018.

[9] H. Liu, H. Xue, Y. Liu, Q. Feng, and L. Li, "Generation of high-order Bessel orbital angular momentum vortex beam using a single-layer reflective metasurface," *IEEE Access*, vol. 8, pp. 126 504–126 510, 2020.

[10] Y. Shen, J. Yang, H. Meng, W. Dou, and S. Hu, "Generating millimeter-wave Bessel beam with orbital angular momentum using reflective-type metasurface inherently integrated with source," *App. Phys. Lett.*, vol. 112, no. 14, 2018.

[11] B. Liu, Y. Cui, and R. Li, "A broadband dual-polarized dual-OAM-mode antenna array for OAM communication," *IEEE Antennas Wireless Propag. Lett.*, vol. 16, pp. 744–747, 2016.

[12] G.-B. Wu, K. F. Chan, and C. H. Chan, "3-D printed terahertz lens to generate higher-order Bessel beams carrying OAM," *IEEE Trans. Antennas Propag.*, 2020, in press. DOI: 10.1109/TAP.2020.3030915.

[13] A. Mazzinghi and A. Freni, "Simultaneous generation of pseudo-Bessel vortex modes with a RLSA," *IEEE Antennas Wireless Propag. Lett.*, vol. 16, pp. 1747–1750, 2017.

[14] D. Comite, G. Valerio, M. Albani, A. Galli, M. Casaletti, and M. Ettorre, "Exciting vorticity through higher-order Bessel beams with a radial-line slot-array antenna," *IEEE Trans. Antennas Propag.*, vol. 65, no. 4, pp. 2123–2128, Feb. 2017.

[15] X. Xu, A. Mazzinghi, A. Freni, and J. Hirokawa, "Simultaneous generation of three OAM modes by using a RLSA fed by a waveguide circuit for 60-GHz-band radiative near-field region OAM multiplexing," *IEEE Trans. Antennas Propag.*, 2020, in press, DOI: 10.1109/TAP.2020.3016428.

[16] D. Comite, W. Fuscaldo, S. Pavone, G. Valerio, M. Ettorre, M. Albani, and A. Galli, "Propagation of nondiffracting pulses carrying orbital angular momentum at microwave frequencies," *App. Phys. Lett.*, vol. 110, no. 11, p. 114102, 2017.

[17] G. Junkin, "A circularly polarized single-frequency multimode helical beam antenna," *IEEE Trans. Antennas Propag.*, vol. 67, no. 3, pp. 1459–1466, Mar. 2018.

[18] G. Junkin, J. Parrón, and A. Tennant, "Characterization of an eight-element circular patch array for helical beam modes," *IEEE Trans. Antennas Propag.*, vol. 67, no. 12, pp. 7348–7355, Dec. 2019.

[19] L. Guan, Z. He, D. Ding, Y. Yu, W. Zhang, and R. Chen, "Polarization-controlled shared-aperture metasurface for generating a vortex beam with different modes," *IEEE Trans. Antennas Propag.*, vol. 66, no. 12, pp. 7455–7459, 2018.

[20] H.-H. Lv, Q.-L. Huang, X.-J. Yi, J.-Q. Hou, and X.-W. Shi, "Low-profile transmitting metasurface using single dielectric substrate for oam generation," *IEEE Antennas Wireless Propag. Lett.*, vol. 19, no. 5, pp. 881–885, 2020.

[21] Z. Zhang, S. Xiao, Y. Li, and B.-Z. Wang, "A circularly polarized multimode patch antenna for the generation of multiple orbital angular momentum modes," *IEEE Antennas Wireless Propag. Lett.*, vol. 16, pp. 521–524, 2016.

[22] Y. Huang, X. Li, Q. Li, Z. Qi, H. Zhu, Z. Akram, and X. Jiang, "Generation of broadband high-purity dual-mode oam beams using a four-feed patch antenna: theory and implementation," *Scientific Rep.*, vol. 9, no. 1, pp. 1–10, 2019.

[23] M. Barbuto, M.-A. Miri, A. Alù, F. Bilotti, and A. Toscano, "A topological design tool for the synthesis of antenna radiation patterns," *IEEE Trans. Antennas Propag.*, vol. 68, no. 3, pp. 1851–1859, Mar. 2019.

[24] J. L. Gómez-Tornero, D. Blanco, E. Rajo-Iglesias, and N. Llombart, "Holographic surface leaky-wave lenses with circularly-polarized focused near-fields–Part I: Concept, design and analysis theory," *IEEE Trans. Antennas Propag.*, vol. 61, no. 7, pp. 3475–3485, Apr. 2013.

[25] W. Fuscaldo, D. Comite, A. Boesso, P. Baccarelli, P. Burghignoli, and A. Galli, "Focusing leaky waves: A class of electromagnetic localized waves with complex spectra," *Phys. Rev. Appl.*, vol. 9, no. 5, p. 054005, 2018.

[26] W. Fuscaldo, A. Benedetti, D. Comite, P. Baccarelli, P. Burghignoli, and A. Galli, "Bessel-Gauss beams through leaky waves: Focusing and diffractive properties," *Phys. Rev. App.*, vol. 13, no. 6, p. 064040, 2020.

[27] P. Burghignoli, W. Fuscaldo, F. Mancini, D. Comite, P. Baccarelli, and A. Galli, "Twisted beams with variable OAM order and consistent beam angle via single uniform circular arrays," *IEEE Access*, vol. 8, pp. 163 006–163 014, 2020.

[28] P. Burghignoli, D. Comite, W. Fuscaldo, P. Baccarelli, and A. Galli, "Higher-order cylindrical leaky waves—part II: Circular array design and validations," *IEEE Trans. Antennas Propag.*, vol. 67, no. 11, pp. 6748–6760, Nov. 2019.

[29] D. Comite, W. Fuscaldo, P. Burghignoli, P. Baccarelli, and A. Galli, "Near-field focusing through higher-order cylindrical leaky waves," in *Proc. 14th European Conf. Antennas Propag.*, 2020, pp. 1–2.

[30] D. Comite, W. Fuscaldo, S. K. Podilchak, P. D. Hilario Re, V. Gómez-Guillamón Buendía, P. Burghignoli, P. Baccarelli, and A. Galli, "Radially periodic leaky-wave antenna for Bessel-beam generation over a wide frequency range," *IEEE Trans. Antennas Propag.*, vol. 66, no. 6, pp. 2828–2843, Jun. 2018.

[31] D. Comite, V. G. Buendía, S. K. Podilchak, D. D. Ruscio, P. Baccarelli, P. Burghignoli, and A. Galli, "Planar antenna design for omnidirectional conical radiation through cylindrical leaky waves," *IEEE Antennas Wireless Propag. Lett.*, vol. 17, no. 10, pp. 1837–1841, Oct. 2018.

[32] D. Blanco, J. L. Gómez-Tornero, E. Rajo-Iglesias, and N. Llombart, "Holographic surface leaky-wave lenses with circularly-polarized focused near-fields–Part II: Experiments and description of frequency steering of focal length," *IEEE Trans. Antennas Propag.*, vol. 61, no. 7, pp. 3486–3494, July 2013.

[33] D. Comite, S. K. Podilchak, M. Kuznetcov, V. G.-G. Buendía, P. Burghignoli, P. Baccarelli, and A. Galli, "Wideband array-fed Fabry-Perot cavity antenna for 2-D beam steering," *IEEE Trans. Antennas Propag.*, vol. 69, no. 2, pp. 784–794, Feb. 2021.

[34] A. F. Morabito, L. Di Donato, and T. Isernia, "Orbital angular momentum antennas: Understanding actual possibilities through the aperture antennas theory," *IEEE Antennas Propag. Mag.*, vol. 60, no. 2, pp. 59–67, Feb. 2018.